




Perspective

# A Short and Practical Overview on Light-Sensing Proteins, Optogenetics, and Fluorescent Biomolecules inside Biomorphs Used as Optical Sensors

Ulises Galindo-García <sup>1</sup>, María Vanegas-Reza <sup>1</sup>, Roberto Arreguín-Espinosa <sup>1</sup> , Karina Sandra Pérez <sup>2</sup> , Ricardo Pérez-Solis <sup>1</sup> , María Eugenia Mendoza <sup>2</sup> , Karla Yadira Cervantes-Quintero <sup>3</sup>, Selene R. Islas <sup>4</sup> , Mayra Cuéllar-Cruz <sup>3</sup>  and Abel Moreno <sup>1,\*</sup> 

- <sup>1</sup> Instituto de Química, Universidad Nacional Autónoma de México, Avenida Universidad 3000, Ciudad de México 04510, México; ulises.galindo@iquimica.unam.mx (U.G.-G.); vanerma05@gmail.com (M.V.-R.); arrespin@unam.mx (R.A.-E.); ricardo.perez@iquimica.unam.mx (R.P.-S.)
- <sup>2</sup> Instituto de Física, Benemérita Universidad Autónoma de Puebla, Avenida San Claudio y 18 Sur, Puebla 72570, México; kperez@ifuap.buap.mx (K.S.P.); emendoza@ifuap.buap.mx (M.E.M.)
- <sup>3</sup> Departamento de Biología, División de Ciencias Naturales y Exactas Campus Guanajuato, Universidad de Guanajuato, Noria Alta S/N, Colonia Noria Alta, Guanajuato 36050, México; ky.cervantes@ugto.mx (K.Y.C.-Q.); mcellar@ugto.mx (M.C.-C.)
- <sup>4</sup> Instituto de Ciencias Aplicadas y Tecnología, Universidad Nacional Autónoma de México, Circuito Exterior S/N, Ciudad Universitaria, México City 04510, México; selene.islas@icat.unam.mx
- \* Correspondence: carcamo@unam.mx; Tel.: +52-55-56224467

**Abstract:** In this contribution, we describe a brief overview of the role of different light-signaling proteins in different biochemical processes (mostly in plants) along the electromagnetic spectrum. We also revise, in terms of perspectives, the applications of all these proteins to optogenetics as a new emerging field of research. In the second part, we present some case studies: First, we used two fluorescent proteins showing an optical response in the green- and red-light wavelengths both isolated from marines' organisms, which were incorporated as light sensors into the silico-carbonate of Ca, Ba, and Sr (usually called biomorphs). The second case study consisted in incorporating phototropins from a plant (*Arabidopsis thaliana*) into the synthesis of biomorphs. Finally, the last part analyses the influence of these three proteins on the shape and structure in the synthesis of silico-carbonates of calcium, barium, and strontium as optical sensors, in order to detect the location of these biomolecules inside these self-assembly crystalline materials called biomorphs.

**Keywords:** phototropins; green light; red- and blue-light photoreceptors; biomorphs; optogenetics



**Citation:** Galindo-García, U.; Vanegas-Reza, M.; Arreguín-Espinosa, R.; Pérez, K.S.; Pérez-Solis, R.; Mendoza, M.E.; Cervantes-Quintero, K.Y.; Islas, S.R.; Cuéllar-Cruz, M.; Moreno, A. A Short and Practical Overview on Light-Sensing Proteins, Optogenetics, and Fluorescent Biomolecules inside Biomorphs Used as Optical Sensors. *Crystals* **2023**, *13*, 1343. <https://doi.org/10.3390/cryst13091343>

Academic Editor: Helmut Cölfen

Received: 27 July 2023

Revised: 23 August 2023

Accepted: 1 September 2023

Published: 3 September 2023



**Copyright:** © 2023 by the authors. Licensee MDPI, Basel, Switzerland. This article is an open access article distributed under the terms and conditions of the Creative Commons Attribution (CC BY) license (<https://creativecommons.org/licenses/by/4.0/>).

## 1. Introduction

Protein photoreceptors are a class of proteins that have an important role in the growth of plants by sensing and responding to light signals [1]. These proteins are responsible for transmitting information about light intensity, direction, and duration to the plant, thus allowing it to adapt to its environment, optimizing its growth and reproduction [2]. The study of plant photoreceptors has been an active area of research in recent decades in which several types of photoreceptors have been identified and characterized [3]. The second type of light-signaling biomolecules is the fluorescent proteins (FPs). These are biological macromolecules that form a fluorophore within their tertiary structure. They have amino acid residues located at positions 65, 66, and 67 of their primary structure that are capable of emitting fluorescence when excited with sufficient energy [4]. Nowadays, 718 fluorescent proteins have been reported in 109 species worldwide, including bacteria, plants, and animals, the majority of which are marine. In total, 80% of these marine organisms belong to the phylum Cnidaria (jellyfish, corals, anemones, zoanthids, etc.). In total, 90% of the proteins obtained within this phylum Cnidaria were described as fluorescent [5]. Though

there has been an increase in the number of studies on the jellyfish *Aequorea victoria* and the green fluorescent protein (GFP) and their applications for biotechnological issues, the studies on their biological role in cnidarians are still few and inconclusive [6]. One of the described functions of FPs is to facilitate or promote the onset of the symbiotic interaction between zooxanthellae and cnidarians by acting as photo-attractors [7]. Other studies in this regard describe that fluorescent protein (FP) and some peptide chromophores (PC) act as photoprotectors of coral tissue [8]. They observed that these molecules are over-expressed as photoprotectors in bleaching events (loss of endosymbionts mainly due to thermal stress conditions and ocean acidification), and in colony growth areas (those with an incipient presence of endosymbionts), since they can absorb the UV radiation to which the internal tissues of corals would be exposed during these phenomena, preventing them from being damaged.

Other groups of light-sensing biomolecules are the phytochromes. These proteins usually appear in two forms named red-light-absorbing phy (Pr) and far-red-light-absorbing phy (Pfr), which have different spectral properties and are interconverted using light [9]. This interconversion allows phytochromes to act as molecular switches, transmitting information about light quality and intensity to a plant [10]. The mechanism by which phytochromes regulate plant growth and development, though not yet fully understood, is thought to involve modulation of gene expression through interactions with other signaling pathways [3]. In addition to phytochromes, plants contain other types of light-sensing biomolecules, including cryptochromes and phototropins, which regulate the different mechanisms involved in plant growth and development [11]. Particularly, the circadian rhythm of plants is regulated by the cryptochromes, whilst phototropins control the direction of plant growth by sensing light's response. The study of plant photoreceptors has significant implications in agriculture and biotechnology, as it has the potential to improve our understanding of plant growth, thus leading to the development of new techniques to optimize crop productivity and yield [12]. For example, manipulation of photoreceptor signaling pathways has been shown to increase crop yield and improve stress tolerance. These findings have the potential to contribute to food security and sustainability [9,13].

There are a variety of light-sensing proteins for specific wavelengths, among them, as previously mentioned, phytochromes are involved in the sensing of infrared and far red light, a very important and characteristic region for plant photoreception and signaling. The blue part of the electromagnetic spectrum is covered by cryptochromes and phototropins that sense blue light, including UV-A and UV-B light [14,15], whereas neochromes, a fusion of phototropins and phytochromes [9], deal with the measurement of blue and red light in an efficient way. Neochromes are chimeric photoreceptors that contain a module of photosensitivity located at the N-terminal, and the entire domains of phototropins at the C-terminal [16]. In evolutionary terms, this photoreception is known to be the product of a common history of genome duplication and expansion. This has shown that phytochromes and phototropins have co-evolved over time through the physical interaction between them in the detection of wavelengths. This has led to the suggestion that plants have evolutionarily found a way to cover almost the entire electromagnetic spectrum, even in the green region where this wavelength was originally thought to be absent [13].

Current investigations have shown that green light is not only important in photosynthesis, but also in physiological responses to the environment. Plants use green light to assimilate carbon dioxide to increase their mass and yield, and to acclimate and adapt to the environment [17]. It is well-known that green light contributes significantly to carbon assimilation and mass gain, but also to the accumulation of biomass in regions where blue and red light do not reach. Green photons also provide a very characteristic signal that depends on the position and orientation of the leaf. This allows the plant to control acclimation more effectively to a fluctuating shade or environment's irradiation as well as increase water use efficiency within the canopy [18,19]. All these photosynthetic organisms collect light through a system of antennae to carry out photochemical reactions [18]. A series of phytochrome-like photoreceptors called cyanochromes (which are photoreceptors

for blue and green light) have recently been discovered. In general terms, green light directs photosynthesis in leaves more efficiently than red light. Finally, photoreceptors involve the participation of many physicochemical conditions and also of proteins that sense these light signals. Recently, some studies have shown that in plants' photobiology, there is a large number of co-regulators as well as internal photoreceptors such as signaling through hormones. These are involved in the perception of unstimulated light (e.g., through thermal changes). Based on all these assumptions, we still have a long way to go to understand the mechanisms at the molecular level that will allow us to connect all the physiological processes [20].

One of the most interesting applications of these light-sensing biomolecules in biomedicine has been focused on optogenetics [21]. The origin of optogenetics dates back to the beginnings of the 1970s when Oesterhelt and Stoerkenius found that the bacterial rhodopsin acted as ion pumps when activated using visible light [22]. Later on, Peter H. Quail used the light-controlled gene promoter based on the plant phytochrome B-Phytochrome interacting with factor 3 (PhyB\_PIF3) photoreceptor system, and this was actually the beginning of optogenetics. In 2005, Boyden and coworkers made the expression of an algal channel rhodopsin. This protein specifically made the neurons respond to light; this was particularly important for the use of light signaling in neuroscience [23]. For the last two decades, optogenetics have used these light-signaling proteins in biomedical research among a variety of other applications [24,25]. The advances in genetic engineering techniques, such as site-directed mutagenesis, have made it possible to create libraries of genetically modified organisms, genes, and proteins [26]. This technique has been applied, for instance, to phototropins to exploit their potential as versatile optogenetic tools in various biochemical applications [27].

In this context, we present several examples to highlight optogenetic results, focused on the importance of photoreceptors, photo-active proteins, and fluorescence proteins in biomedical sciences. Protein tyrosine phosphatase 1B (PTP1B) is of great importance as a regulator in cancer and diabetes studies. Its catalytic activity can be effectively modulated by coupling it to LOV2 from *Avena sativa* (AsLOV2), using the  $\alpha 7$  helix enzymes of PTP1B to interact with the C-terminal of LOV2. This coupling creates a photosensitive structure that undergoes chain disruption upon irradiation with blue light. The resulting photoinduced changes in the C- and N-terminals profoundly affect the conformation of the protein, thereby compromising the catalytic activity of the enzyme during the day and in dark states [28]. In addition, the remarkable rapid and reversible properties of *Avena sativa* LOV2 have been exploited as an effector in engineered shuttling proteins, allowing precise control of nucleocytoplasmic transport through affinity changes between light and dark states [29]. One notable method for protein isolation involves the use of the light-switchable monobody H4A attached to AsLOV2. The monobody-LOV system binds to the SH2 domain of proteins in dark conditions and releases them in the light state, providing a versatile tool for precise control of their binding affinities [30]. Photoswitches have become valuable tools in medicine, particularly in the development of novel phototoxic therapies [31]. One of the examples is the activation of a mini reactor, by using a blue laser light, composed of encapsulins with a fluorescent protein photosensitizer derived from *Arabidopsis thaliana* LOV2 (AtLOV2) [32]. This innovative mini reactor effectively generates reactive oxygen species that have a toxic effect on tumor cells, showing great promise in advanced photodynamic cancer therapies [33,34]. In addition, in the context of breast cancer progression, optogenetic engineering of the NOTCH1 receptor has provided insights into its role in the intricate NOTCH signaling pathway. This receptor is important in the pathogenesis of several diseases, including breast cancer progression. Light activation of the NOTCH1 receptor has revealed its involvement in chemoresistance, cell proliferation, and spheroid growth in breast cancer cells, further highlighting the complexity of NOTCH signaling in disease pathogenesis [34].

The quest to repair the human body, particularly the heart, is a critical goal in medical research. Unlike some species, humans are unable to regenerate damaged hearts, which can

have a profound impact on their lifespan. However, recent advances in optogenetic tools have opened a promising avenue for promoting cardiac regeneration. By modifying the Yes-associated protein with the AsLOV2 domain, it is possible to induce reparative genetic programs in response to light activation. This innovative approach holds great potential for the development of less invasive therapies targeting human cardiomyocytes, opening up new opportunities to enhance cardiac repair and to improve patient outcomes [35,36].

In addition, the LOV domain from *Rhodobacter sphaeroides* was used [37] to regulate bacterial cell division in *Escherichia coli* by modifying its gene expression system. This light-activated gene expression system uses a repressor based on the LOV domain. In dark conditions, the repressor forms dimers that inhibit promoter activity, effectively repressing gene expression. However, upon exposure to light, the repressor dimers dissociate, initiating gene expression [38]. On the other hand, rhodopsins, like phototropins, have proven to be versatile and valuable tools in biological research when using photoreceptors. The effect of blue light on cell proliferation was studied, and mouse embryonic stem cells were virally infected to express channelrhodopsin-2 (ChR2) with green fluorescent protein (GFP). Optical stimulation disrupted cell cycle progression, leading to a shift from self-renewal to differentiation [39,40]. However, microbial rhodopsins have an absorption spectrum of the retina, which is extremely sensitive to the local chemical and electrostatic environment and extremely useful for optogenetic applications. These proteins working as actuators sense the neuronal activity in the brain [41,42]. In general, rhodopsins are classified as photoactive proteins containing a retinal chromophore in animals and microbes. Particularly, the transport of ions either in a passive or active manner and channels activated using light or light-driven channel pumps are the main tools used in optogenetics. These channels usually are related to the transport along with the absorption color, ion selectivity, and open/close dynamics. Since 2005, one of these channels was used as a neural excitation tool for applications in optogenetics. In general, we can say that channels are usually more efficient tools than pumps for multiple ion permeation [43].

Another important photoactive protein is the Photoactive Yellow Protein usually called PYP. This is a small water-soluble protein with a cysteine linked to a p-coumaric acid chromophore. In optogenetics, this protein can be used as a tunable optical switch because blue light triggers trans to cis isomerization of the chromophore and production of a light state with altered conformational dynamics. Based on this property, PYP has been used as switchable protein in optogenetics and it is usually linked to effector domains resulting in soluble, well-behaved constructs [44,45]. This feasibility to form specific constructs has been used to design structure-based photoswitchable affibody scaffolds for applications in immunochemistry, particularly in the use of antibodies using the tunable properties of the PYP-Z-domain with a light-dependent binding in vitro and in vivo [46]. There are other proteins useful for optogenetics' applications, for instance, the near-infrared fluorescent proteins used as biosensors. These phytochromes use their feasibility for light-controlled cell signaling, gene expression, and protein localization [47].

Nowadays, there is an emerging new field of research called optobiochemistry. This focuses on the control of protein functions in living cells in spatio-temporal resolution given by photons. Light-sensitive proteins have been used as optobiochemical tools to module diverse protein functions. Light induction is used on the interaction between plant phytochromes and their binding partner to regulate fused protein domains via light-induced oligomerization, heterodimerization, dissociation, and conformational changes with optical control. In general terms, there is a confusion in terminology with optogenetics. Properly speaking, optobiochemistry uses light to control biochemical processes in the cell contrary to optogenetics because photons are not modulating genes [48].

In the first part of this contribution, we describe a brief overview of the role of proteins from different types of light signaling along the electromagnetic spectrum. In the second part as case studies, we used two proteins showing an optical response in the green- and red-light wavelengths both isolated from marines' organisms. These were incorporated as light sensors into the silico-carbonate of Ca, Ba, and Sr (usually called biomorphs). The

second case study is the incorporation of phototropins from plants (*Arabidopsis thaliana*) into the biomorphs. Finally, the last part deals with the analysis of the influence of these three proteins on the shape and on the structure in the synthesis of silico-carbonates of calcium, barium, and strontium as optical sensors, in order to detect the location of these biomolecules inside these self-assembly crystalline materials called biomorphs.

## 2. Materials and Methods

### 2.1. Protein Isolation and Purification

These photoreceptors (green/red) from marines' organisms were isolated and purified. They showed an optical response in the following regions: 495–570 nm (green) and 620–700 nm for red. The third case is the photodetection in the blue wavelength (phototropins from plants); it was 450–500 nm.

#### 2.1.1. Phototropins

The macromolecular complex phototropin (FT-blue thereafter) shows a response to unidirectional blue light, a mechanism associated with the light's conversion into chemical energy through signal transduction and oligomerization. In our experiments, we used PHOT1 from *Arabidopsis thaliana*, which is characterized for containing two LOV domains with a flavin mononucleotide (FMN) chromophore ea., responsible for the blue-light absorption. The PHOT1 was cloned in PET-32a(+) using a BgIII/EcoRI plasmid. Protein over-expression was performed using *E. coli* (TOP10 strain). The strain was grown in an LB Broth supplemented with 100 µg/mL of ampicillin, and the experiments were performed at 37 °C, keeping a constant shaking of 200 rpm. An LB broth supplemented with 2% agar and ampicillin was used for bacterial growth in a solid medium. In total, 5 mL of the cell culture after 12 h of pre-inoculation was added to 150 mL of liquid LB for inoculation; when optical density reached a value between 0.5 and 0.8, we induced the overexpression with 0.05 mM of isopropyl β-D-1-thiogalactopyranoside (IPTG) for 22 h. After this process, samples were centrifugated at 4500 rpm × 10 min and washed three times with PBS. Cellular lysis was performed by using an ultrasonic cell disruptor MISONIX SONICATOR 3000 Vernon Hills (IL, USA), working at 20 kHz during 10 min of alternating 10/30 s pulses—on/off. To remove cell debris, the homogenized dispersion was centrifuged at 5000 rpm for 10 min at 4 °C. The concentration of the protein was determined with spectrophotometry. According to the protein purification procedure, we performed two types of chromatography techniques: (i) affinity and (ii) size exclusion. By using affinity chromatography, 5 mL of the protein supernatant at 50 mg/mL was uploaded to a HisTrap™ HP affinity column Cytiva™ Marlborough (MA, USA), previously equilibrated with a lysis buffer. The column was washed with a phosphate buffer (20 mM of sodium phosphate, 500 mM of sodium chloride, and 20 mM of imidazole; pH 7.4). The resin bound to the protein was eluted with 5 mL of an elution buffer (20 mM of sodium phosphate, 500 mM of sodium chloride, and 500 mM of imidazole; pH 7.4). Collected fractions of 0.5 mL were taken to the next step. Aliquots of 30 µL were taken from the cellular homogenized part as well as those of the supernatant and fractions bound to the column. All these samples were analyzed with the gel electrophoresis technique using 12% (*w/v*) polyacrylamide-SDS gels (SDS-PAGE). This SDS-PAGE was performed to evaluate the induction time and purity of the obtained protein. The fraction containing the protein of interest was then concentrated using Amicon® Miami (FL, USA) 50 kDa centrifugal filters Merck Millipore™ Temecula, (CA, USA). From the concentrated protein, 0.5 mL aliquots at a concentration of 5 mg/mL were injected onto an analytical molecular size exclusion column Superdex™ 75 Increase 10/300 GL Cytiva™ Marlborough (MA, USA), GE Healthcare Chicago (IL, USA), previously equilibrated with a 2.5 CV citrate buffer (50 mM of sodium citrate dihydrate; 150 mM of sodium chloride; pH 4.0), in the ÄKTA pure™ Marlborough (MA, USA) chromatography system Cytiva™ Marlborough (MA, USA), GE Healthcare, Chicago (IL, USA). A flow rate of 0.5 mL/min of the citrate buffer

was used to dissolve the sample using the isocratic method. Absorbance at 280 nm was used to read the chromatograms. All reagents were of a Sigma molecular biology grade.

### 2.1.2. Green-Light and Red-Light Signaling Protein from *Condylactis gigantea*

All animal studies complied with the international and national protocols: ARRIVE (US), The Care and Use of Laboratory Animals (NIH-US), and the Ethical Use of Animals for Experimentation at the Universidad Nacional Autónoma de México (UNAM) (Mexico City, Mexico). The Dirección General de Ordenación Pesquera y Acuicultura, Quintana Roo, México granted us the permit No. PPF-066/20 to collect *Condylactis gigantea*. It is important to remark that a sea anemone collection as well as extract specimens of *C. gigantea* were obtained from the reef lagoon at Puerto Morelos, Quintana Roo, México (20.880232, −86.861239 and 20.867966, −86.866335) from between 5 and 8 m deep, with the help of a chisel, hammer, and SCUBA diving. In total, 19 specimens were extracted, 10 green and 9 magenta. For transfer to the laboratory, each specimen was placed in a hermetically sealed bag with seawater from the collection site and stored in a larger volume container at room temperature. Once in the laboratory, the residues of the marine substrate and sediments that remained adhered to each organism were removed, preserving their immersion in the collected seawater.

Each specimen of *Condylactis gigantea*, free of sediment, was extracted from the seawater collected, drained, and subjected to two surface rinses, using one volume of deionized water equivalent to the volume of each organism. The aqueous extract obtained presented the characteristic color of the phenotype of each organism: magenta or green. Finally, the extracts were combined maintaining the differentiation by color, lyophilized, and stored deep-frozen at −60 °C.

Fractionation of the aqueous extract used 2.33 mg of protein from the green aqueous extract, quantified with the BCA methodology. This portion of the extract was fractionated using a Hi Prep QFF 16/10 anion exchange column, with a total volume of 20 mL, in an ÄKTA®-FPLC unit. Mobile phase A was as follows: Tris-HCl (20 mM) at pH 8.0 with exchange to B—Tris-HCl (20 mM) at pH 8.0 + NaCl (1 M)—with a flow rate of 2 mL/min, with gradients isocratic of solution A for the first 25 min, increasing to 50% B at min 75, and finally isocratic to 100% B for 20 min. The chromatogram was obtained with the absorbance reading at 280 nm. From this procedure, 11 fractions were obtained that were reduced to a volume of 300 mL using a modular refrigerated vacuum concentrator, SpeedVac® New York (NY, USA). For the characterization, UV-Visible and Fluorescence Spectroscopy was used. Each of the 11 fractions obtained with ion exchange chromatography were evaluated as emitters of fluorescence, in a 1 × 1 × 3 cm quartz cell, adding 2.2 mL of deionized water to complete the cell volume for the readings. The analysis of the UV-Visible light spectrum was measured in Varian-Cary-50Bio® Palo Alto (CA, USA) equipment. Finally, the fluorescence excitation and emission spectra were obtained with Varian-Cary-Eclipse® equipment Palo Alto (CA, USA), with Scan Version 1.1 (132) software.

## 2.2. Synthesis of Silica–Carbonate of Alkaline Metals (Biomorphs)

Crystalline aggregates of induced morphology, usually called biomorphs, are auto-organized materials that in general display a variety of morphologies that mimic living forms. These biomorphs show characteristic curvatures, semi-spheres, leaf-like shapes, and a variety of characteristic morphologies. These seem to be unrestricted from the classic symmetry in crystallography [49]. Silica–carbonate biomorphs were successfully synthesized through the gas diffusion method [50,51] with some modifications as in the protocol of synthesis published in [51]. All reagents were of an analytical grade from Merck (St. Louis, MO, USA) to perform the experiments.

### 2.3. Characterization of Biomorphs

#### 2.3.1. Scanning Electron Microscopy

After coating with a thin gold layer using an SPI-coater, the SEM microphotographs of biomorphs were collected using a scanning electron microscope (SEM) from TESCAN (Brno, Czech Republic) model VEGA3 SB. All details about sample preparation, imaging acquisition, and data analyses were performed following the procedure published by Cuéllar-Cruz et al., 2022 [51].

#### 2.3.2. Raman Spectroscopy

For the Raman characterization, a confocal Raman microscope, WITec model alpha300 RA, was used (WITec GmbH, Ulm, Germany). In most of the cases, we used 672 lines per millimeter. A green laser light excitation of 532 nm was used (Nd:YVO<sub>4</sub>). The incident laser contained a power of 14.4 mW focused using 20×, 50×, and 100× objectives (Zeiss, Germany) with 0.4, 0.75, and 0.9 NA, respectively. The spectra were collected with the following characteristics: 0.5 s integration and 10 accumulations. The data processing and analysis were obtained with WITec Project FIVE Version 5.1 software.

#### 2.3.3. Confocal Microscopy

This confocal microscopy was carried out using a Zeiss LSM700 (Germany, Europe) scanning laser confocal system including an inverted Axio Observer Z1 microscope coupled to the software Zen 2011 SP3 black edition (version 8.1). Biomorph images were acquired using Differential Interference Contrast (DIC) microscopy for the brightfield. Wavelengths employed to detect fluorescent signals of biomorph–protein complexes were as follows: FT-blue (excitation, 405 nm, and emission, 435 nm), cgigGFP (excitation, 488 nm, and emission, 518 nm), and cgigRF (excitation, 555 nm, and emission, 585 nm). The objective employed was N-Achroplan63X/0.85. Images were obtained using Z-stack series with a slice thickness of 1 µm.

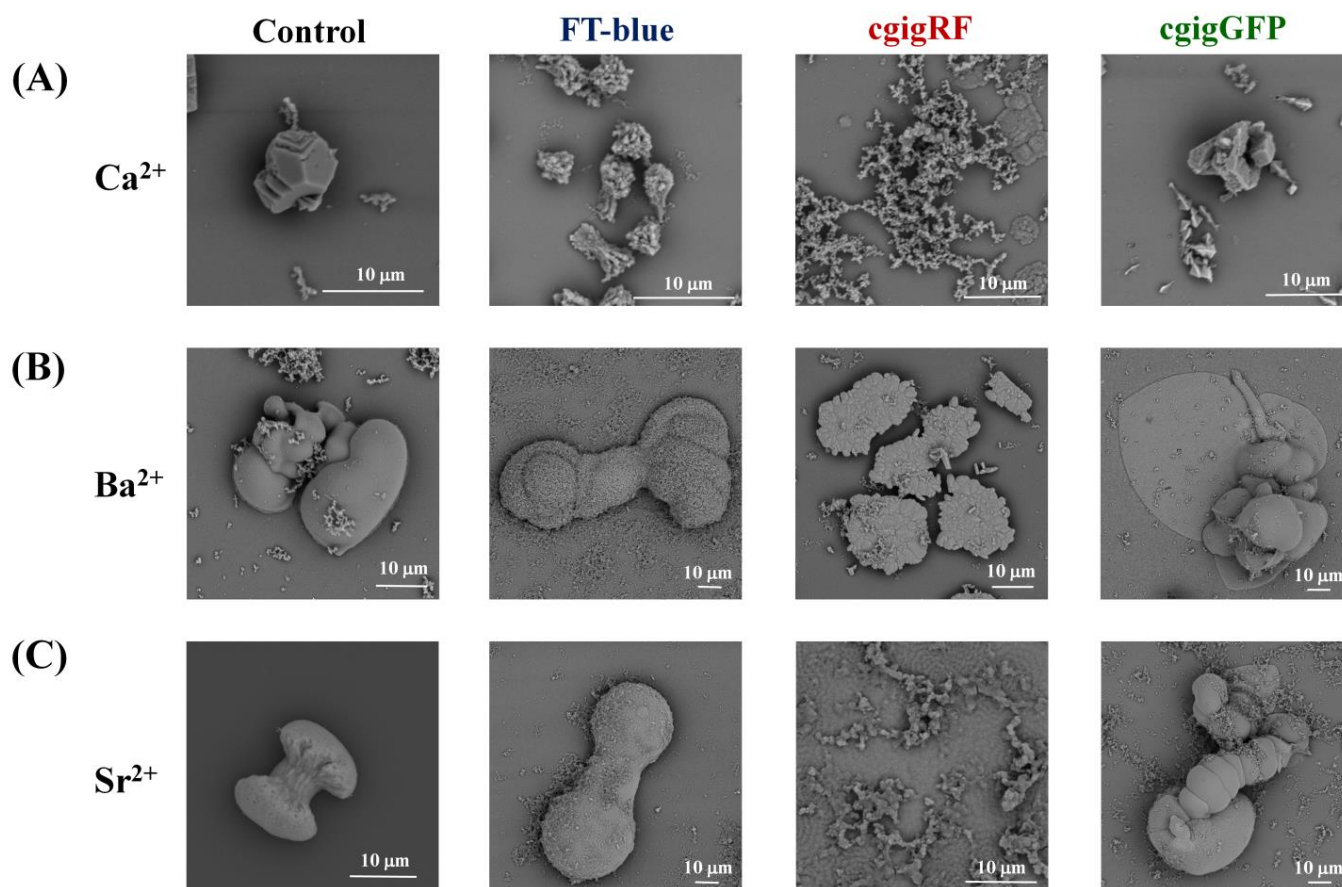
## 3. Results and Discussion

### *Proteins in Action, Working as Optical Sensors Inside Biomorphs*

Three proteins with specific photosensitivity were isolated and purified with the idea of employing them as optical sensors to determine their location within biomorphs at different wavelengths. These biomorphs have been extensively studied on prebiotic chemistry in the origin of life [49,51]. Having proteins as optical sensors covering most of the regions of the electromagnetic spectrum will, in a near future, allow us to suggest chemical and physiological mechanisms to explain the role of photodetection in plants and the role that these proteins play in the applications to optogenetics in biomedical sciences. The fluorophores of the two fractions used for the formation of biomorphs presented a maxima fluorescence emission at 498 nm and 678 nm, which correspond to the green fluorescent protein cgigGFP [52] and the second to the red-light mixture of porphyrins (chlorophyll-*a*, chlorophyll-*b*, and phaeophytin-*a*), respectively. The fluorescence emission in the blue 435 nm was obtained using the phototropins (FT-blue) from *Arabidopsis thaliana*. For this protein, which was over-expressed, for this contribution, we obtained a maximum emission between 435 and 450 nm.

Once the absorption and emission spectra for each protein were obtained and incorporated into the synthesis of biomorphs, scanning electron microscopy (SEM) was carried out to evaluate changes on the morphology of the biomorphs. This shows how the proteins were selectively incorporated into the biomorphs at specific locations, and how some have influenced the morphology of the biomorphs. The analysis of the SEM micrographs visually showed a strong influence of cgigRF on these biomorphs, modifying the morphology completely (Figure 1). However, at present, we do not have any X-ray crystalline structure available of this protein that suggests a biochemical mechanism (chemical recognition) based on the 3D structure. The micrographs show a general trend collected along the glass plate, though we were unable to point out the exact location of the proteins inside the

self-assembly crystalline materials (biomorphs). This led us to perform a more precise characterization using confocal microscopy.

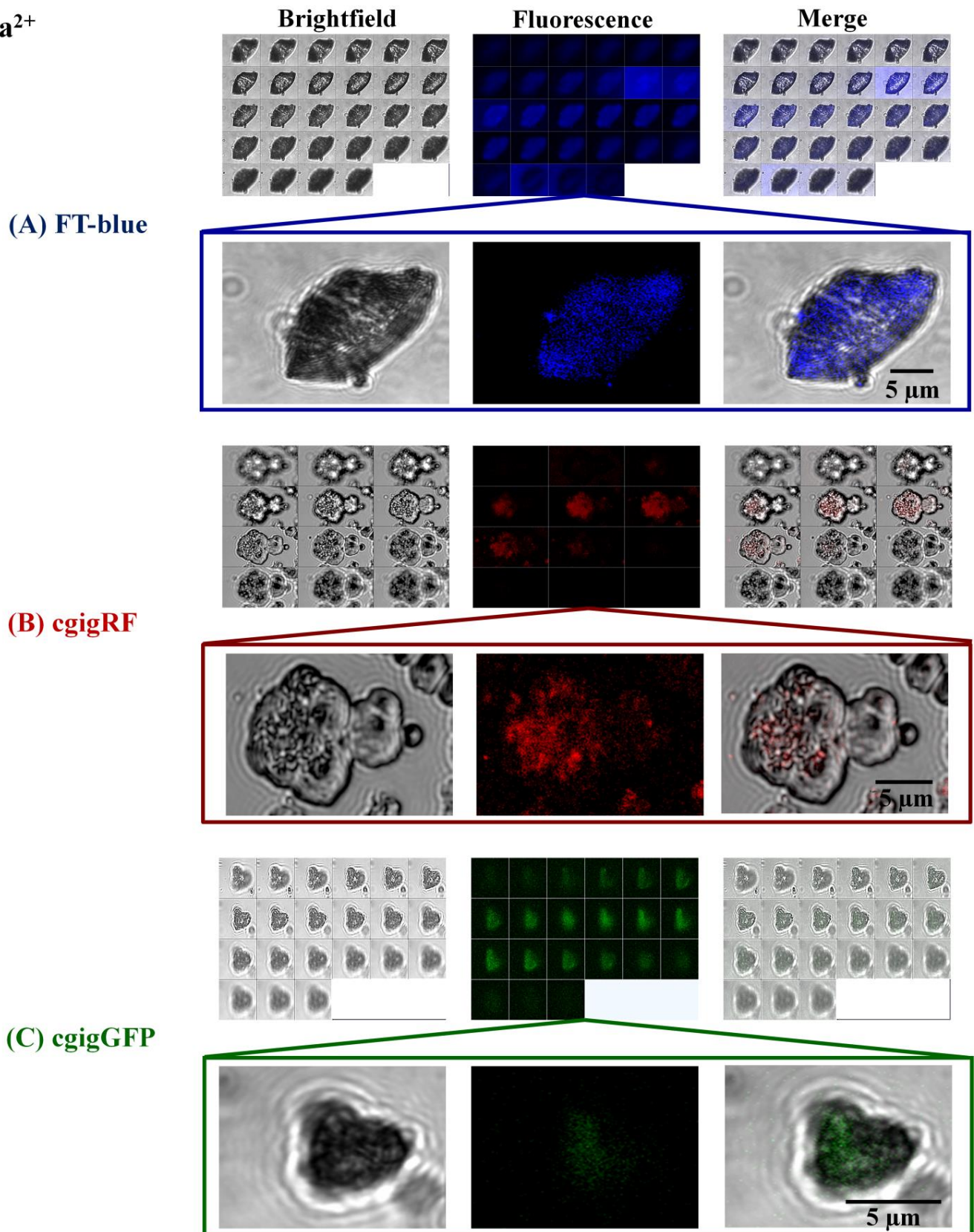


**Figure 1.** SEM images of the synthesized biomorphs containing the proteins are shown for each alkaline metal used: (A)  $\text{Ca}^{2+}$ , (B)  $\text{Ba}^{2+}$ , and (C)  $\text{Sr}^{2+}$ . The code on the upper part corresponding to FT-blue is the phototropin, cgigRF is the red-light protein, and cgigGFP corresponds to the green-fluorescence protein.

The use of existing fluorescence techniques like confocal microscopy is useful in the characterization of these complex samples. However, it was through confocal spectroscopy that we were able to observe these proteins within the structure of biomorphs in different sectors (areas) of the crystalline structures. The proteins were emulating the signaling role that could be played in plant leaves. For the calcium silico-carbonate biomorphs, the proteins are practically able to internalize inside the biomorph (Figure 2) and in the case of FT-blue and cgigGFP (green), they are part of the whole structure (Figures 2A and 3C). The barium silico-carbonate biomorphs obtained from the addition of the FT-blue protein are observed to be located only on the outside of the biomorph (Figure 3A). In contrast, the cgigRF or cgigGFP proteins are located inside the biomorph structure (Figure 3B,C).

These data indicate that the alkaline earth metals are important in the interaction with the protein. For calcium silico-carbonate biomorphs, the proteins were practically able to internalize inside the biomorph whereas in the case of FT-blue and cgigGFP, they were part of the whole structure (Figure 2). However, in the case of barium silico-carbonate biomorphs, the proteins were practically only found in a small part of the biomorph, but not in the whole structure (Figure 3). This result is particularly important, as it seems there is a selective location of the protein and a specific interaction with the biomorph structure.



$\text{Ca}^{2+}$ 

**Figure 2.** Images of calcium silico-carbonate biomorphs synthesized with the proteins: (A) FT-blue; (B) cgigRF; and (C) cgigGFP obtained with brightfield and confocal microscopy with different zooming.

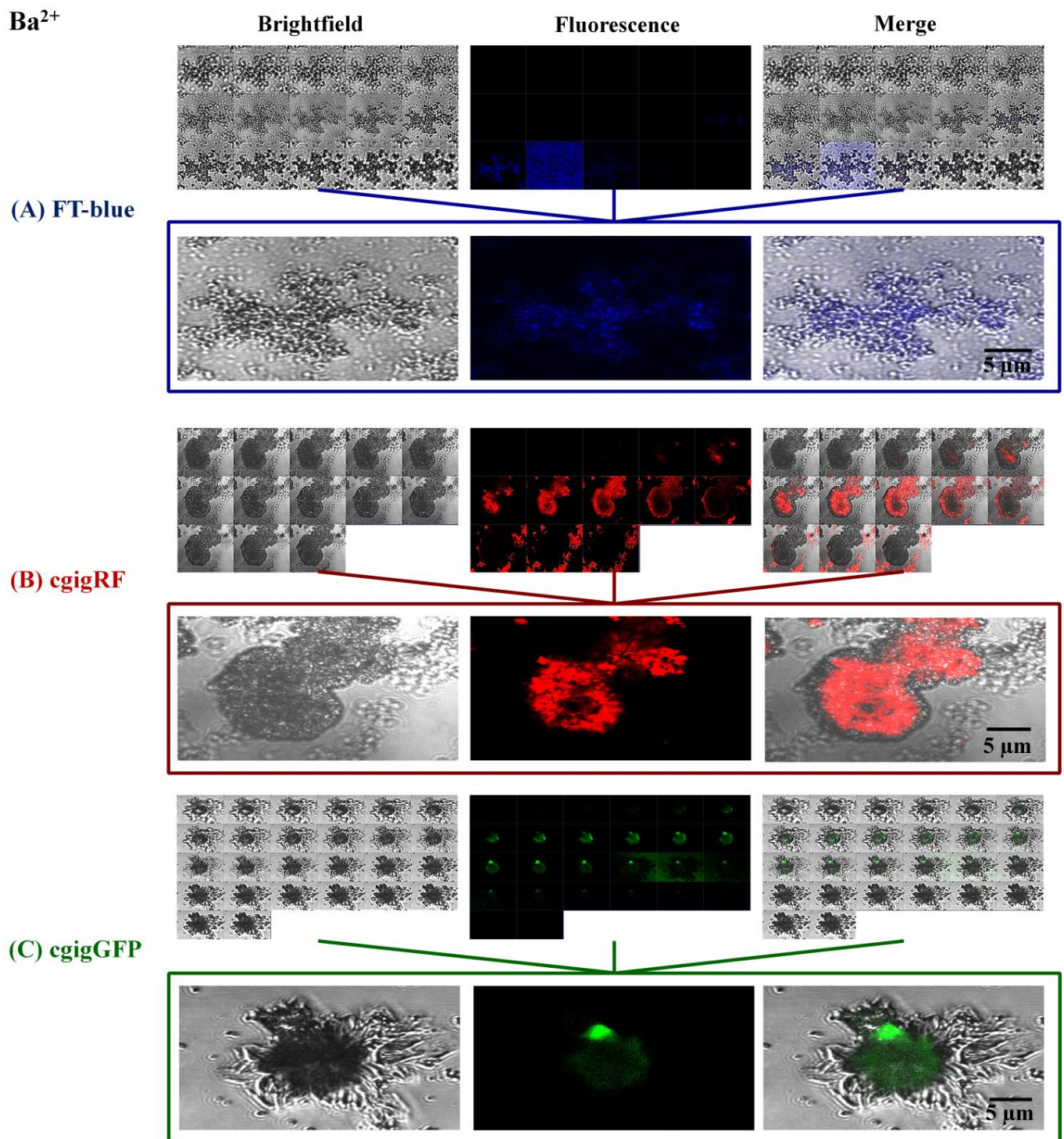


**Figure 3.** Representative confocal images of barium silico-carbonate biomorphs synthesized in the presence of the proteins (A) FT-blue; (B) cgigRF; and (C) cgigGFP. The microphotographs were obtained with brightfield and confocal microscopy with different zooming.

For the case of silico-carbonates of strontium, optical sectioning was performed on several biomorphs. In this case, the biomorphs with the FT-blue protein were found to be localized inside the biomorphs (Figure 4A). Biomorphs in the presence of the cgigRF or cgigGFP proteins localize in virtually the entire biomorph structure (Figure 4B,C).

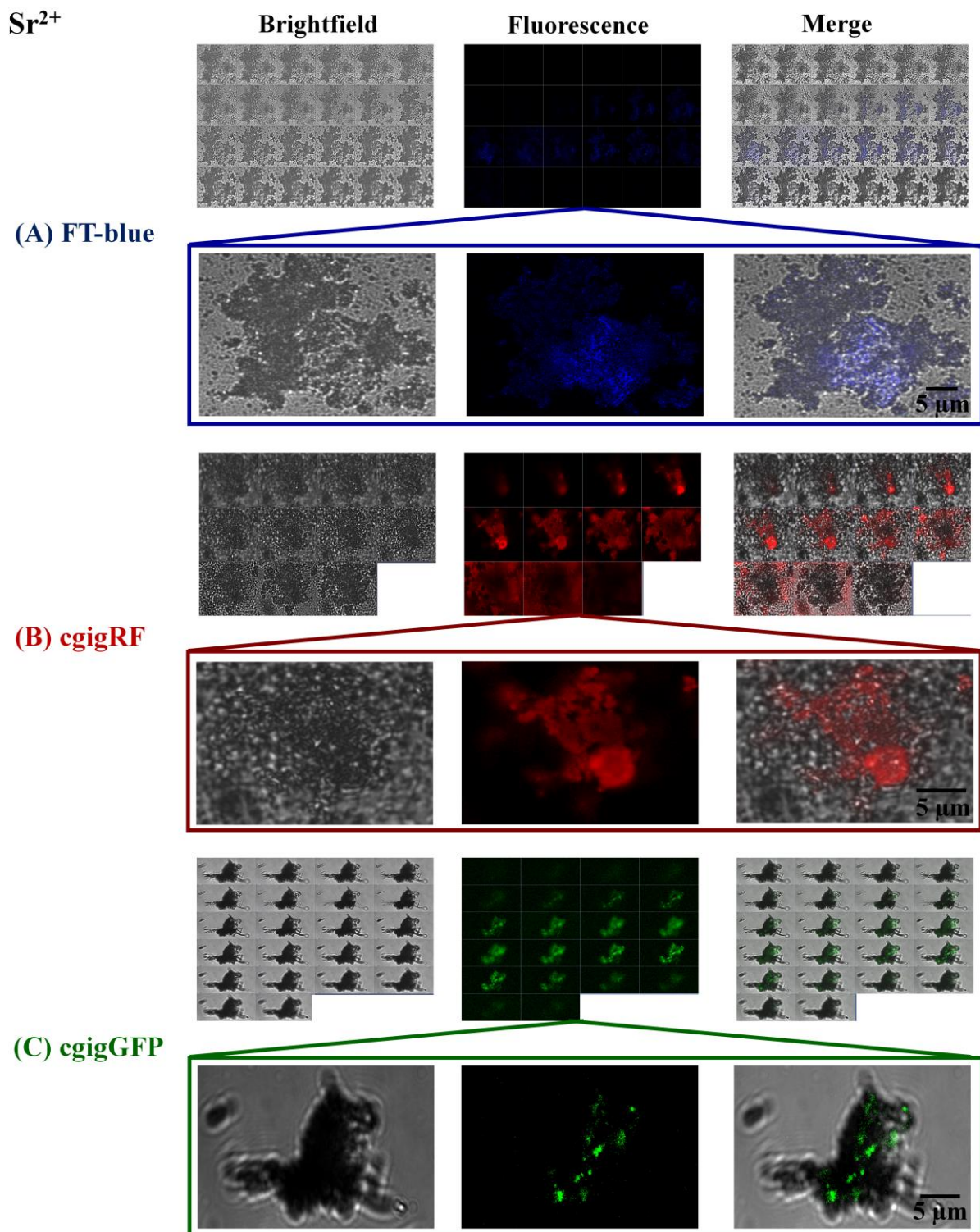


**Figure 4.** Confocal images of strontium silico-carbonate biomorphs synthesized in the presence of (A) FT-blue; (B) cgigRF; or (C) cgigGFP. The micrographs were obtained with brightfield and confocal microscopy with different zooming.

Data generally showed that morphology was dependent on the type of alkaline metal (Ca, Ba, or Sr) as well as on specific protein. That helped to determine the preference of biomorphs for one or another protein, though sometimes the same proteins would either surround the biomorphs or be internalized inside the crystalline structure. The chemical

and structural interactions of biomorphs with FT-blue, cgigGFP, and cgigRF proteins were performed with Raman spectroscopy. This technique has already proved to be reliable and powerful in the identification of polymorphs in biomorphs, just like those obtained with X-ray diffraction techniques at synchrotron facilities [53]. As shown in Table 1—the Raman spectra from the control (biomorphs with  $\text{Ca}^{2+}$ )—the peaks were identified at 156, 282, 711, and  $1085\text{ cm}^{-1}$ , and these corresponded to the calcite polymorph with a trigonal P3-m structure of  $\text{CaCO}_3$  [54,55]. In the case of the spectra of the biomorphs in the presence of the FT-blue or cgigRF protein, the calcite polymorph was also identified (see the characteristic bands reported in Table 1). For cgigGFP protein/biomorphs, the major peaks were found at 113, 302, 754, and  $1089\text{ cm}^{-1}$  (Table 1), and they corresponded to  $\text{CaCO}_3$ , but in its aragonite polymorph [56]. These results indicate that the cgigGFP protein apparently has the ability to modify the crystal structure of  $\text{CaCO}_3$ , leading to one or another polymorph.

**Table 1.** Raman spectroscopy of silica–carbonate biomorphs and the polymorphs found in the synthesis.

Type of Synthesis	Protein	Raman ( $\text{cm}^{-1}$ )	Composition
$\text{Ca}^{2+}$	Control	156, 282, 711, 1085	Calcite
	FT-blue	155, 281, 750, 1084	Calcite
	cgigRF	156, 280, 711, 1084	Calcite
	cgigGFP	113, 302, 754, 1089	Aragonite
$\text{Ba}^{2+}$	Control	91, 137, 153, 224, 689, 1057	Witherite
	FT-blue	99, 140, 151, 233, 695, 1059, 1455, 2852	Witherite
	cgigRF	93, 140, 154, 222, 690, 1058, 2939	Witherite
	cgigGFP	95, 132, 223, 690, 1058, 1503, 2860	Witherite
$\text{Sr}^{2+}$	Control	151, 184, 700, 1072	Strontianite
	FT-blue	112, 150, 183, 252, 700, 1072, 1443, 1616, 2936	Strontianite
	cgigRF	109, 148, 180, 700, 1072, 2948	Strontianite
	cgigGFP	112, 150, 181, 699, 1071, 2929	Strontianite

In the case of the biomorphs from barium obtained with or without the proteins, the composition and crystalline structures were also determined with Raman spectroscopy. For the control sample, the Raman peaks were identified at 91, 137, 153, 224, 689, and  $1057\text{ cm}^{-1}$  (Table 1). For  $\text{BaCO}_3$ , the peaks corresponded to its aragonite-type crystal structure, called witherite [56]. Additionally, barium silico-carbonate synthesized in the presence of FT-blue, cgigRF, or cgigGFP was identified with peaks corresponding to the witherite polymorph, as in the control biomorphs (Table 1). This result is interesting, because it shows that even though the crystalline habit of the barium silico-carbonate biomorphs is not modified in the presence of any of these three proteins, the morphology they adopt does vary among the protein involved during their synthesis.

The characterization and the chemical composition of the silica–carbonate biomorphs of strontium (Sr) were also performed with Raman spectroscopy. The control sample showed peaks at 151, 184, 700, and  $1072\text{ cm}^{-1}$  (Table 1). These signals corresponded to  $\text{SrCO}_3$  in its strontianite crystal structure (aragonite-type) and belonged to the orthorhombic space group [57]. In the case of the strontium silico-carbonate biomorphs synthesized with FT-blue, cgigRF, or cgigGFP, the characteristic peaks from Raman spectra of  $\text{SrCO}_3$  with the strontianite crystal structure (Table 1) were similar to those found for the control biomorphs. As was observed for the barium silico-carbonates in the presence of the different proteins, the strontium biomorphs synthesized containing these biomolecules did show a typical morphology of biomorphs published elsewhere (Figure 1), but without changing the crystalline habit. This indicates that each protein according to its amino acid composition influences the adopted biomorphs' morphology.

It was observed that the morphology of biomorphs is protein-dependent, which suggests that the interaction of each protein in the structure that determines the final morphology of the biomorph is different. Thus, there are two possibilities of participation of each protein with the biomorph structure: (i) the protein can be integrated inside the crystalline structure of the biomorph, or (ii) it can be located on the external part of the biomorph, acting as a protein coat. In order to evaluate the type of participation of each protein in the structure of the biomorphs, they were visualized and analyzed with confocal microscopy. Biomorphs with and without proteins were evaluated for the three silico-carbonates: (i)  $\text{Ca}^{2+}$ , (ii)  $\text{Ba}^{2+}$ , and (iii)  $\text{Sr}^{2+}$ . One of the applications of these contributions is to have a wider possibility of incorporating fluorescent proteins at the inner/outer structure of biomorphs to light them at different types of wavelengths. The importance of plants in the detection of different wavelengths has turned them into experts with highly efficient systems and detectors or specific optical sensors, which they have achieved through evolution. However, this opportunity should be exploited further into different applications, as we have shown in medical sciences with optogenetics or in the use of photosensitive proteins to determine their location in complex systems such as biomorphs.

Finally, it is difficult to isolate, purify, and structurally resolve via an X-ray or any other crystallographic technique the entire complex light-sensing system in plants. Many of the proteins are cell membrane proteins that are difficult to crystallize. As reported in this overview article, it is possible to have data on some structures that have been solved and to have some of the biological and physiological mechanisms of light assimilation, but in many of the cases, there are not enough structures available in databases such as the PDB (Protein Data Bank).

#### 4. Conclusions

This contribution showed that photodetection at different wavelengths has served plants along evolution to optimize the capture of photons in a wide range of wavelengths of the electromagnetic spectrum. Even wavelengths that were apparently unimportant (e.g., green light) play a very important role in photodetection for very specific physiological functions in plants. The existence of photosensitive proteins found not only in plants but also in marine systems has demonstrated the potential of light photoreceptors. One of the important applications for all this knowledge of bio-photosensors will certainly be focused in optogenetics, where even specific proteins (from marine organisms) or plant photoreceptors (phototropins) can be used as optical sensors (photo-switches) for different applications as shown for the case of biomorphs. Finally, modern greenhouses that produce various foods (fruits, vegetables, and legumes) could increase their efficiency by using different wavelengths at the same time. In the near future, the light assimilation mechanisms of plants will be a biomimetic strategy to be used in various applications such as the examples mentioned in this overview article.

**Author Contributions:** Conceptualization, M.E.M., A.M., U.G.-G. and K.S.P.; methodology, M.C.-C., K.S.P., M.V.-R., R.A.-E., K.Y.C.-Q., R.P.-S. and S.R.I.; validation, A.M. and M.C.-C.; formal analysis, A.M.; investigation, all authors; resources, A.M. and M.E.M.; writing—original draft preparation, A.M.; writing—review and editing, A.M. and M.C.-C.; supervision, A.M.; project administration, A.M. and M.C.-C. All authors have read and agreed to the published version of the manuscript.

**Funding:** This research was funded by CONAHCYT—the project number A1-S-7509 and project CF-2019/39216 (DGAPA UNAM Project PAPIIT, No. IN207922).

**Acknowledgments:** The authors of this contribution acknowledge the support from different projects to complete this research. Ulises Galindo-García (CVU 488998) and Karina S. Pérez (CVU 271764) acknowledge CONAHCYT for the postdoctoral fellowship at the Instituto de Química, UNAM (U.G.-G.) and Estancias Posdoctorales por México para la Consolidación de las y los Investigadores por México (K.S.P.). Abel Moreno (A.M.) thanks CONAHCYT (project number: A1-S-7509) for the support of this work related to phototropins and DGAPA-UNAM PAPIIT Project IN207922 for fluorescent proteins in biomedicine. This work was carried out with the financial support granted

to Mayra Cuéllar-Cruz with Project No. CF2019-39216 from the *Consejo Nacional de Humanidades, Ciencias y Tecnologías* (CONAHCYT) and *Proyecto-Institucional-UGTO-002/2023* from *Universidad de Guanajuato*, Mexico. The authors thank *Laboratorio Universitario de Caracterización Espectroscópica* (LUCE) of the *Instituto de Ciencias Aplicadas y Tecnología*, UNAM for the support for the Raman measurements. The authors thank *Laboratorio de Microscopía Confocal del Departamento de Biología de la Universidad de Guanajuato* for their support for microphotographs. The authors acknowledge Antonia Sánchez-Marín for the English revision and correction of the final version of this contribution.

**Conflicts of Interest:** The authors declare no conflict of interest.

## References

1. Griffin, J.H.C.; Toledo-Ortiz, G. Plant photoreceptors and their signalling components in chloroplastic anterograde and retrograde communication. *J. Exp. Bot.* **2022**, *73*, 7126–7138. [[CrossRef](#)]
2. Haga, K.; Sakai, T. Photosensory adaptation mechanisms in hypocotyl phototropism: How plants recognize the direction of a light source. *J. Exp. Bot.* **2023**, *74*, 1758–1769. [[CrossRef](#)]
3. Kong, S.-G.; Okajima, K. Diverse photoreceptors and light responses in plants. *J. Plant Res.* **2016**, *129*, 111–114. [[CrossRef](#)]
4. Chudakov, D.M.; Matz, M.V.; Lukyanov, S.; Lukyanov, K.A. Fluorescent Proteins and their applications in imaging living cells and tissues. *Physiol. Rev.* **2010**, *90*, 1103–1163. [[CrossRef](#)]
5. Lambert, T.J. FPbase: A community-editable fluorescent protein database. *Nat. Methods* **2019**, *16*, 277–278. [[CrossRef](#)]
6. Deo, S.K.; Daunert, S. Luminescent proteins from *Aequorea victoria*: Applications in drug discovery and in high throughput analysis. *Anal. Bioanal. Chem.* **2001**, *369*, 258–266. [[CrossRef](#)]
7. Aihara, Y.; Maruyama, S.; Baird, A.H.; Iguchi, A.; Takahashi, S.; Minagawa, J. Green fluorescence from cnidarian hosts attracts symbiotic algae. *Proc. Natl. Acad. Sci. USA* **2019**, *116*, 2118–2123. [[CrossRef](#)]
8. Kusmita, L.; Edi, A.N.P.; Franyoto, Y.D.; Mutmainah; Haryanti, S.; Nurcahyanti, A.D.R. Sun protection and antibacterial activities of carotenoids from the soft coral *Sinularia* sp. symbiotic bacteria from Panjang Island, North Java Sea. *Saudi Pharm. J.* **2023**, *31*, 101680. [[CrossRef](#)]
9. Casal, J.J. Phytochromes, cryptochromes, phototropin: Photoreceptor interactions in plants. *Photochem. Photobiol.* **2000**, *71*, 1–11. [[CrossRef](#)]
10. Cheng, M.-C.; Kathare, P.K.; Paik, I.; Huq, E. Phytochrome signaling networks. *Annu. Rev. Plant Biol.* **2021**, *72*, 217–244. [[CrossRef](#)]
11. Briggs, W.R.; Huala, E. Blue-Light Photoreceptors in Higher Plants. *Annu. Rev. Cell Dev. Biol.* **1999**, *15*, 33–62. [[CrossRef](#)]
12. Cordeiro, A.M.; Andrade, L.; Monteiro, C.C.; Leitão, G.; Wigge, P.A.; Saibo, N.J.M. Phytochrome-interacting factors: A promising tool to improve crop productivity. *J. Exp. Bot.* **2022**, *73*, 3881–3897. [[CrossRef](#)]
13. Li, F.-W.; Mathews, S. Evolutionary aspects of plant photoreceptors. *J. Plant Res.* **2016**, *129*, 115–122. [[CrossRef](#)]
14. Villafani, Y.; Yang, H.W.; Park, Y.-I. Color sensing and signal transmission diversity of cyanobacterial phytochromes and cyanobacteriochromes. *Mol. Cells* **2020**, *43*, 509–516.
15. Kami, C.; Lorrain, S.; Hornitschek, P.; Fankhauser, C. Light-regulated plant growth and development. *Curr. Top. Dev. Biol.* **2010**, *91*, 29–66.
16. Masamitsu, W. Chimera photoreceptor, neochrome, has arisen twice during plant evolution. *Tanpakushitsu Kakusan Koso. Protein Nucleic Acid Enzym.* **2006**, *51*, 1580–1589.
17. Smith, H.L.; McAusland, L.; Murchie, E.H. Don't ignore the green light: Exploring diverse roles in plant processes. *J. Exp. Bot.* **2017**, *68*, 2099–2110. [[CrossRef](#)]
18. Wang, W.; Yu, L.-J.; Xu, C.; Tomizaki, T.; Zhao, S.; Umena, Y.; Chen, X.; Qin, X.; Xin, Y.; Suga, M.; et al. Structural basis for blue-green light harvesting and energy dissipation in diatoms. *Science* **2019**, *363*, eaav0365. [[CrossRef](#)]
19. Willmer, C.M.; Johnston, W.R. Carbon dioxide assimilation in some aerial plant organs and tissues. *Planta* **1976**, *130*, 33–37. [[CrossRef](#)]
20. Paik, I.; Huq, E. Plant photoreceptors: Multi-functional sensory proteins and their signaling networks. *Semin. Cell Dev. Biol.* **2019**, *92*, 114–121. [[CrossRef](#)]
21. Neghab, H.K.; Soheilifar, M.H.; Grusch, M.; Ortega, M.M.; Djavid, G.E.; Saboury, A.A.; Goliaei, B. The state of the art of biomedical applications of optogenetics. *Lasers Surg. Med.* **2022**, *54*, 202–216. [[CrossRef](#)] [[PubMed](#)]
22. Oesterhelt, D.; Stoekenius, W. Rhodopsin-like Protein from the Purple Membrane of *Halobacterium halobium*. *Nat. New Biol.* **1971**, *233*, 149–152. [[CrossRef](#)]
23. Boyden, E.S.; Zhang, F.; Bamberg, E.; Nagel, G.; Deisseroth, K. Millisecond-timescale, genetically targeted optical control of neural activity. *Nat. Neurosci.* **2005**, *8*, 1263–1268. [[CrossRef](#)]
24. Katz, Y.; Sokoletsky, M.; Lampl, I. In-vivo optogenetics and pharmacology in deep intracellular recordings. *J. Neurosci. Methods* **2019**, *325*, 108324. [[CrossRef](#)]
25. Sureda-Vives, M.; Sarkisyan, K.S. Bioluminescence-Driven Optogenetics. *Life* **2020**, *10*, 318. [[CrossRef](#)] [[PubMed](#)]
26. Konrad, K.R.; Gao, S.; Zurbriggen, M.D.; Nagel, G. Optogenetic Methods in Plant Biology. *Annu. Rev. Plant Biol.* **2023**, *74*, 313–339. [[CrossRef](#)] [[PubMed](#)]

27. Espinosa-Juárez, J.V.; Chiquete, E.; Estañol, B.; Aceves, J.d.J. Optogenetic and Chemogenic Control of Pain Signaling: Molecular Markers. *Int. J. Mol. Sci.* **2023**, *24*, 10220. [[CrossRef](#)] [[PubMed](#)]
28. Zimmerman, S.; Kuhlman, B.; Yumerefendi, H. Engineering and Application of LOV2-Based Photoswitches. *Methods Enzymol.* **2016**, *580*, 169–190. [[CrossRef](#)] [[PubMed](#)]
29. Hongdusit, A.; Zwart, P.H.; Sankaran, B.; Fox, J.M. Minimally disruptive optical control of protein tyrosine phosphatase 1B. *Nat. Commun.* **2020**, *11*, 788. [[CrossRef](#)]
30. Carrasco-López, C.; Zhao, E.M.; Gil, A.A.; Alam, N.; Toettcher, J.E.; Avalos, J.L. Development of light-responsive protein binding in the monobody non-immunoglobulin scaffold. *Nat. Commun.* **2020**, *11*, 4045. [[CrossRef](#)]
31. Chen, H.; Wu, F.; Xie, X.; Wang, W.; Li, Q.; Tu, L.; Li, B.; Kong, X.; Chang, Y. Hybrid Nanoplatfrom: Enabling a Precise Antitumor Strategy via Dual-Modal Imaging-Guided Photodynamic/Chemo-/Immunosynergistic Therapy. *ACS Nano* **2021**, *15*, 20643–20655. [[CrossRef](#)] [[PubMed](#)]
32. Chmelyuk, N.S.; Oda, V.V.; Gabashvili, A.N.; Abakumov, M.A. Encapsulins: Structure, Properties, and Biotechnological Applications. *Biochemistry* **2023**, *88*, 35–49. [[CrossRef](#)] [[PubMed](#)]
33. Kałafut, J.; Czapiński, J.; Przybyszewska-Podstawka, A.; Czerwonka, A.; Odrzywolski, A.; Sahlgren, C.; Rivero-Müller, A. Optogenetic control of NOTCH1 signaling. *Cell Commun. Signal.* **2022**, *20*, 67. [[CrossRef](#)] [[PubMed](#)]
34. Adams, D.S.; Tseng, A.-S.; Levin, M. Light-activation of the Archaeorhodopsin H<sup>+</sup>-pump reverses age-dependent loss of vertebrate regeneration: Sparking system-level controls in vivo. *Biol. Open* **2013**, *2*, 306–313. [[CrossRef](#)] [[PubMed](#)]
35. Toh, P.J.Y.; Lai, J.K.H.; Hermann, A.; Destaing, O.; Sheetz, M.P.; Sudol, M.; Saunders, T.E. Optogenetic control of YAP cellular localisation and function. *EMBO Rep.* **2022**, *23*, e54401. [[CrossRef](#)]
36. Toh, P.J.Y.; Sudol, M.; Saunders, T.E. Optogenetic control of YAP can enhance the rate of wound healing. *Cell. Mol. Biol. Lett.* **2023**, *28*, 39. [[CrossRef](#)]
37. Conrad, K.S.; Bilwes, A.M.; Crane, B.R. Light-Induced Subunit Dissociation by a Light–Oxygen–Voltage Domain Photoreceptor from *Rhodobacter sphaeroides*. *Biochemistry* **2013**, *52*, 378–391. [[CrossRef](#)]
38. Camsund, D.; Lindblad, P.; Jaramillo, A. Genetically engineered light sensors for control of bacterial gene expression. *Biotechnol. J.* **2011**, *6*, 826–836. [[CrossRef](#)]
39. Zhou, Y.; Kong, D.; Wang, X.; Yu, G.; Wu, X.; Guan, N.; Weber, W.; Ye, H. A small and highly sensitive red/far-red optogenetic switch for applications in mammals. *Nat. Biotechnol.* **2022**, *40*, 262–272. [[CrossRef](#)]
40. Reshetnikov, V.V.; Smolskaya, S.V.; Feoktistova, S.G.; Verkhusha, V.V. Optogenetic approaches in biotechnology and biomaterials. *Trends Biotechnol.* **2022**, *40*, 858–874. [[CrossRef](#)]
41. McIsaac, R.S.; Bedbrook, C.N.; Arnold, F.H. Recent advances in engineering microbial rhodopsins for optogenetics. *Curr. Opin. Struct. Biol.* **2015**, *33*, 8–15. [[CrossRef](#)] [[PubMed](#)]
42. Brinks, D.; Adam, Y.; Kheifets, S.; Cohen, A.E. Painting with Rainbows: Patterning light space, time, and wavelength for multiphoton optogenetic sensing control. *Acc. Chem. Res.* **2016**, *49*, 2518–2526. [[CrossRef](#)] [[PubMed](#)]
43. Kandori, H. Retinal Proteins: Photochemistry and Optogenetics. *Bull. Chem. Soc. Jpn.* **2020**, *93*, 76–85. [[CrossRef](#)]
44. Brechun, K.E.; Zhen, D.; Jaikaran, A.S.I.; Borisenko, V.; Kumauchi, M.; Hoff, W.D.; Arndt, K.M.; Woolley, G.A. Detection of Incorporation of *p*-Coumaric Acid into Photoactive Yellow Protein Variants in Vivo. *Biochemistry* **2019**, *58*, 2682–2694. [[CrossRef](#)]
45. Romei, M.G.; Lin, C.-Y.; Boxer, S.G. Structural and spectroscopic characterization of photoactive yellow protein and photo-switchable fluorescent protein constructs containing heavy atoms. *J. Photochem. Photobiol. A Chem.* **2020**, *401*, 112738. [[CrossRef](#)] [[PubMed](#)]
46. Woloschuk, R.M.; Reed, P.M.; Jaikaran, A.S.; Demmans, K.Z.; Youn, J.; Kanelis, V.; Uppalapati, M.; Woolley, G.A. Structure-based design of photoswitchable affibody scaffold. *Protein Sci.* **2021**, *30*, 2359. [[CrossRef](#)]
47. Chernov, K.G.; Redchuk, T.A.; Omelina, E.S.; Verkhusha, V.V. Near-infrared fluorescent proteins, biosensors, and optogenic tools engineered from phytochromes. *Chem. Rev.* **2017**, *117*, 6423. [[CrossRef](#)]
48. Seong, J.; Lin, M.Z. Optobiochemistry: Genetically encoded control of protein activity by light. *Annu. Rev. Biochem.* **2021**, *90*, 475–501. [[CrossRef](#)]
49. García-Ruiz, J.M.; van Zuilen, M.A.; Bach, W. Mineral self-organization on a lifeless planet. *Phys. Life Rev.* **2020**, *34–35*, 62–82. [[CrossRef](#)]
50. Noorduyn, W.L.; Grinthal, A.; Mahadevan, L.; Aizenberg, J. rationally designed complex, hierarchical microarchitectures. *Science* **2013**, *340*, 832–837. [[CrossRef](#)]
51. Cuéllar-Cruz, M.; Islas, S.R.; Ramírez-Ramírez, N.; Pedraza-Reyes, M.; Moreno, A. Protection of the DNA from selected species of five kingdoms in nature by Ba(II), Sr(II), and Ca(II) Silica-Carbonates: Implications about biogenicity and evolving from prebiotic chemistry to biological chemistry. *ACS Omega* **2022**, *7*, 37410–37426. [[CrossRef](#)]
52. Labas, Y.A.; Gurskaya, N.G.; Yanushevich, Y.G.; Fradkov, A.F.; Lukyanov, K.A.; Lukyanov, S.A.; Matz, M.V. Diversity and evolution of the green fluorescent protein family. *Proc. Natl. Acad. Sci. USA* **2002**, *99*, 4256–4261. [[CrossRef](#)]
53. Cuéllar-Cruz, M. Influence of abiotic factors in the chemical origin of life: Biomorphs as a study model. *ACS Omega* **2021**, *6*, 8754–8763. [[CrossRef](#)]
54. Vagenas, N.V.; Gatsouli, A.; Kontoyannis, C.G. Quantitative analysis of synthetic calcium carbonate polymorphs using FT-IR spectroscopy. *Talanta* **2003**, *59*, 831–836. [[CrossRef](#)] [[PubMed](#)]

55. Agarwal, P.; Berglund, K.A. In Situ Monitoring of Calcium Carbonate Polymorphs during batch crystallization in the presence of polymeric additives Using Raman Spectroscopy. *Cryst. Growth Des.* **2003**, *3*, 941–946. [[CrossRef](#)]
56. Lin, C.-C.; Liu, L.-G. High-pressure Raman spectroscopic study of post-aragonite phase transition in witherite (BaCO<sub>3</sub>). *Eur. J. Miner.* **1997**, *9*, 785–792. [[CrossRef](#)]
57. Buzgar, N.; Apopei, A.I. The Raman study of certain carbonates. *Geologie* **2009**, *2*, 97–112.

**Disclaimer/Publisher’s Note:** The statements, opinions and data contained in all publications are solely those of the individual author(s) and contributor(s) and not of MDPI and/or the editor(s). MDPI and/or the editor(s) disclaim responsibility for any injury to people or property resulting from any ideas, methods, instructions or products referred to in the content.